



Article

# The CaSR Modulator NPS-2143 Reduced UV-Induced DNA Damage in Skh:hr1 Hairless Mice but Minimally Inhibited Skin Tumours

Chen Yang <sup>1</sup>, Mark Stephen Rybchyn <sup>1,2</sup> , Warusavithana Gunawardena Manori De Silva <sup>1</sup>, Jim Matthews <sup>3</sup>, Katie Marie Dixon <sup>1</sup>, Andrew J. A. Holland <sup>4</sup> , Arthur David Conigrave <sup>5</sup> and Rebecca Sara Mason <sup>1,5,\*</sup>

<sup>1</sup> School of Medical Sciences and Bosch Institute, University of Sydney, Sydney, NSW 2006, Australia

<sup>2</sup> School of Chemical Engineering, University of New South Wales, Sydney, NSW 2033, Australia

<sup>3</sup> Sydney Informatics Hub, University of Sydney, Sydney, NSW 2008, Australia

<sup>4</sup> Douglas Cohen Department of Paediatric Surgery, The Children's Hospital at Westmead Clinical School, The Faculty of Medicine and Health, The University of Sydney, Sydney, NSW 2145, Australia

<sup>5</sup> School of Life and Environmental Sciences, Charles Perkins Centre (D17), University of Sydney, Sydney, NSW 2006, Australia

\* Correspondence: rebecca.mason@sydney.edu.au

**Abstract:** The calcium-sensing receptor (CaSR) is an important regulator of epidermal function. We previously reported that knockdown of the CaSR or treatment with its negative allosteric modulator, NPS-2143, significantly reduced UV-induced DNA damage, a key factor in skin cancer development. We subsequently wanted to test whether topical NPS-2143 could also reduce UV-DNA damage, immune suppression, or skin tumour development in mice. In this study, topical application of NPS-2143 (228 or 2280 pmol/cm<sup>2</sup>) to Skh:hr1 female mice reduced UV-induced cyclobutane pyrimidine dimers (CPD) ( $p < 0.05$ ) and oxidative DNA damage (8-OHdG) ( $p < 0.05$ ) to a similar extent as the known photoprotective agent 1,25(OH)<sub>2</sub> vitamin D<sub>3</sub> (calcitriol, 1,25D). Topical NPS-2143 failed to rescue UV-induced immunosuppression in a contact hypersensitivity study. In a chronic UV photocarcinogenesis protocol, topical NPS-2143 reduced squamous cell carcinomas for only up to 24 weeks ( $p < 0.02$ ) but had no other effect on skin tumour development. In human keratinocytes, 1,25D, which protected mice from UV-induced skin tumours, significantly reduced UV-upregulated p-CREB expression ( $p < 0.01$ ), a potential early anti-tumour marker, while NPS-2143 had no effect. This result, together with the failure to reduce UV-induced immunosuppression, may explain why the reduction in UV-DNA damage in mice with NPS-2143 was not sufficient to inhibit skin tumour formation.

**Keywords:** ultraviolet radiation (UV); photoprotection; 1,25-dihydroxyvitamin D<sub>3</sub> (1,25D); cyclobutane pyrimidine dimer (CPD); 8-hydroxy-2'-deoxyguanosine (8-OHdG); calcium sensing receptor (CaSR); photocarcinogenesis; cyclic AMP response element binding factor (CREB); squamous cell carcinoma (SCC)



**Citation:** Yang, C.; Rybchyn, M.S.; De Silva, W.G.M.; Matthews, J.; Dixon, K.M.; Holland, A.J.A.; Conigrave, A.D.; Mason, R.S. The CaSR Modulator NPS-2143 Reduced UV-Induced DNA Damage in Skh:hr1 Hairless Mice but Minimally Inhibited Skin Tumours. *Int. J. Mol. Sci.* **2023**, *24*, 4921. <https://doi.org/10.3390/ijms24054921>

Academic Editor: Ingolf Bernhardt

Received: 15 December 2022

Revised: 20 February 2023

Accepted: 21 February 2023

Published: 3 March 2023



**Copyright:** © 2023 by the authors. Licensee MDPI, Basel, Switzerland. This article is an open access article distributed under the terms and conditions of the Creative Commons Attribution (CC BY) license (<https://creativecommons.org/licenses/by/4.0/>).

## 1. Introduction

Skin cancers can be categorized into three main types: (i) basal cell carcinoma (BCC); (ii) squamous cell carcinoma (SCC), both of which arise from keratinocytes; and (iii) melanoma. Pathological changes in skin, including ultraviolet radiation (UV)-induced DNA damage [1–3], mutagenesis [4], inflammation [5], and immunosuppression [6,7] can ultimately lead to photocarcinogenesis. UV not only directly induces DNA lesions such as cyclobutane pyrimidine dimers (CPDs) and (6–4) photoproducts [8], but also induces indirect biological damage targeting DNA, protein, and lipids via the production of reactive oxygen species (ROS) and nitric oxide products, forming 8-hydroxy-2'-deoxyguanosine (8-OHdG) as a marker of oxidative DNA damage [9]. UV has potent immunosuppressive effects that promote tumour development [7,10–12].

Repetitive UV-induced epidermal thickening and pigmentation production together protected mice [13] and humans from subsequent UV challenges, with 75% less erythema and 60% less DNA damage in skin [14,15]. This thickening of the skin as a result of keratinocyte differentiation and may be more protective than melanogenesis (pigmentation production) in response to UV, at least in some populations [16]. Calcium concentration is believed to act as a switcher between proliferation and differentiation of keratinocytes [17]. This is consistent with a well-defined gradient for total calcium that increases from the basal to the outermost layers of the epidermis [18]. The responses of keratinocytes to extracellular calcium ion concentrations ( $\text{Ca}^{2+}_o$ ) and the maintenance of systemic calcium homeostasis are mainly controlled by the calcium-sensing receptor (CaSR), a member of family C of the G protein-coupled receptors (GPCR) [19,20]. There are commercially available small molecule allosteric agents, for example, NPS-2143 works as an antagonist that reduces CaSR activity to block the increase of  $\text{Ca}^{2+}_i$  [21–25]. NPS-2143 has been used in an attempt to promote a brief secretion of parathyroid hormone in plasma for treatment of osteoporosis [22]. Previously we reported that CaSR knockdown or exposure to the CaSR negative allosteric modulator NPS-2143 protected human keratinocytes in culture against UV-induced DNA damage at a similar level to the known photoprotective agent, 1,25-dihydroxyvitamin D<sub>3</sub> (1,25D) [26]. This photoprotective activity of NPS-2143 was attributed at least in part to enhanced DNA repair and to reduction in ROS [26].

Immunosuppression, along with UV-induced DNA lesions, is a key factor leading to photocarcinogenesis [27]. Topical 1,25D has been shown to protect mice from UV-induced CPDs, apoptotic sunburn cells, and UV-induced immunosuppression, and to reduce UV-induced skin tumours [28–31] as well as chemically-induced skin tumours [32]. The use of albino hairless (Skh:hr1) mice exposed to chronic UV is accepted as a reliable model of photocarcinogenesis [33–35]. While cultured primary keratinocytes provide a powerful approach for studying epidermal biology, they imperfectly model the multi-cell types and structural order of living epidermis [36]. Thus we aimed to investigate, for the first time in a mouse model, whether manipulation of the CaSR by its negative allosteric modulator NPS-2143 would protect against DNA damage in mouse epidermis after acute UV exposure. We also wanted to examine if topical treatment of NPS-2143 would reduce UV-induced skin inflammation and immune suppression, as well as in response to a chronic UV-exposure, whether it would reduce UV-induced skin tumours in comparison with the positive control, 1,25D.

## 2. Results

### 2.1. NPS-2143 Protects against DNA Damage and Apoptotic Keratinocytes in Skh:hr1 Mice

Acute UV irradiation generated CPDs, oxidative DNA damage 8-OHdG (Figure 1), and sunburn cells (Figure 2) in mouse skin. The photoprotective hormonal form of vitamin D, 1,25D [29,37–41], was used as the positive control in these experiments. All agents in all experiments were applied topically immediately after exposure to solar-simulated UV (ssUV). Minimal staining in SHAM skin, particularly of 8-OHdG, indicates basal damage of the nuclei. In female mice, topical NPS-2143 at 2 concentrations, 228 pmol/cm<sup>2</sup> and 2280 pmol/cm<sup>2</sup> effectively reduced both CPD ( $p < 0.05$ ,  $F(2.062, 19.25) = 15.64$ ) and 8-OHdG ( $p < 0.05$ ,  $F(1.537, 11.78) = 34.58$ ) (Figure 1a–d). Topical NPS-2143 also reduced UV-induced sunburn cells ( $p < 0.01$ ,  $F(2.044, 15.67) = 32.04$ ) which are apoptotic keratinocytes with characteristic pyknotic nuclei and eosinophilic cytoplasm [42] (Figure 2a,b).

In male Skh:hr1 mice, significant reduction in UV-induced CPD was only seen after treatment with a high dose of NPS-2143, 2280 pmol/cm<sup>2</sup> ( $p < 0.01$ ,  $F(2.190, 18.98) = 6.738$ ) (Figure 1e–h). Both concentrations of this agent, however, as well as 1,25D, significantly protected against oxidative DNA damage, 8-OHdG ( $p < 0.01$ ,  $F(1.284, 14.55) = 8.726$ ), in males (Figure 1f,h), and against sunburn cells ( $p < 0.01$ ,  $F(2.663, 33.74) = 53.07$ ) (Figure 2c,d).

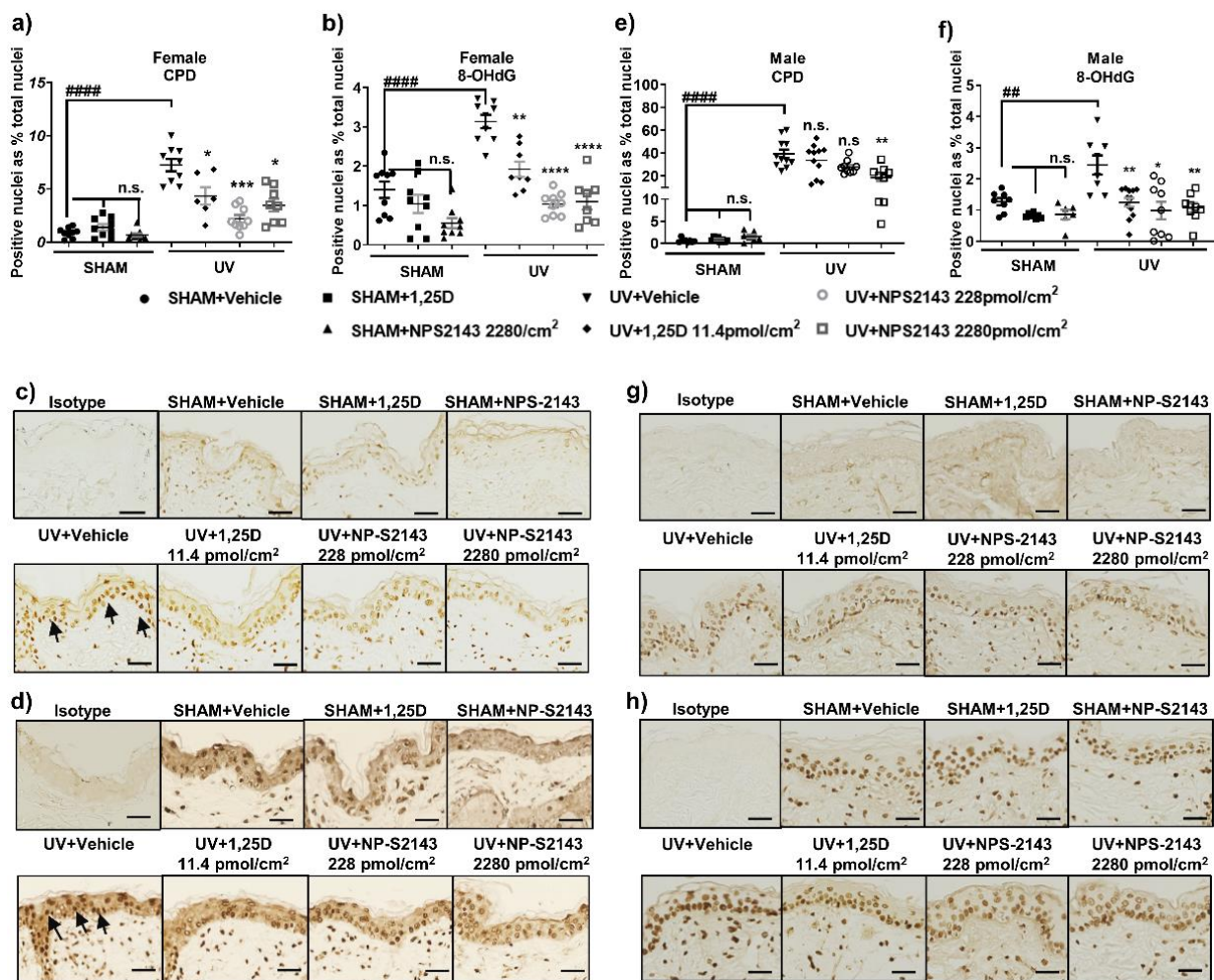


**Figure 1.** NPS-2143 inhibits DNA damage in female and male mouse skin following acute UV irradiation. Immediately after exposure to ssUV, female and male Skh:hr1 mice were treated with vehicle 1,25D (11.4 pmol/cm<sup>2</sup>) or NPS-2143 (228 or 2280 pmol/cm<sup>2</sup>) topically and the skin was harvested after 3 h. DNA damage is shown in graphs for CPD in female (a) or male (e) mice and 8-OHdG in female (b) or male (f) mice with graphs displaying data as dot plots. These graphs show representative data from a minimum of two individual experiments with similar results on each occasion. \*\*\*\*  $p < 0.0001$ , \*\*\*  $p < 0.001$ , \*\*  $p < 0.01$ , \*  $p < 0.05$ , and n.s. not significant, when compared with UV-vehicle treated group by linear mixed model analysis; ##  $p < 0.01$ , ####  $p < 0.0001$  significantly different from sham vehicle by  $t$ -test (a):  $t = 6.088$ ,  $df = 10$  (b):  $t = 5.385$ ,  $df = 10$  (c):  $t = 6.084$ ,  $df = 13$ , (d):  $t = 2.728$ ,  $df = 10$ .  $n = 9$  (triplicate biopsies per mice, 3 mice per group). Photomicrographs show UV-induced CPD in female (c) or male (g) mice and 8-OHdG in female (d) or male (h) mice. Black arrows point to the dark brown staining in nuclei indicating the presence of DNA damage. Scale bar = 100  $\mu$ m.

## 2.2. NPS-2143 Effects on Inflammatory Response after ssUV and on Contact Hypersensitivity in Female Mice

After exposure to 3 minimal erythral doses (MED) of solar-simulated UV, where a MED is defined as the lowest dose of UV which produces a mild reddening of the skin at 24 h, the mice developed skin edema [31]. In this study, skinfold thickness increased daily, reaching a maximum at day 4 post-UV, then decreased gradually (Figure 3a). On the 4th day, UV-induced edema was significantly reduced in the presence of 1,25D (11.4 pmol/cm<sup>2</sup>) ( $p < 0.05$ ) or NPS-2143 (2280 pmol/cm<sup>2</sup>) ( $p < 0.05$ ), compared to the vehicle-treated control mice ( $F(1.531,9.187) = 8.857$ ).

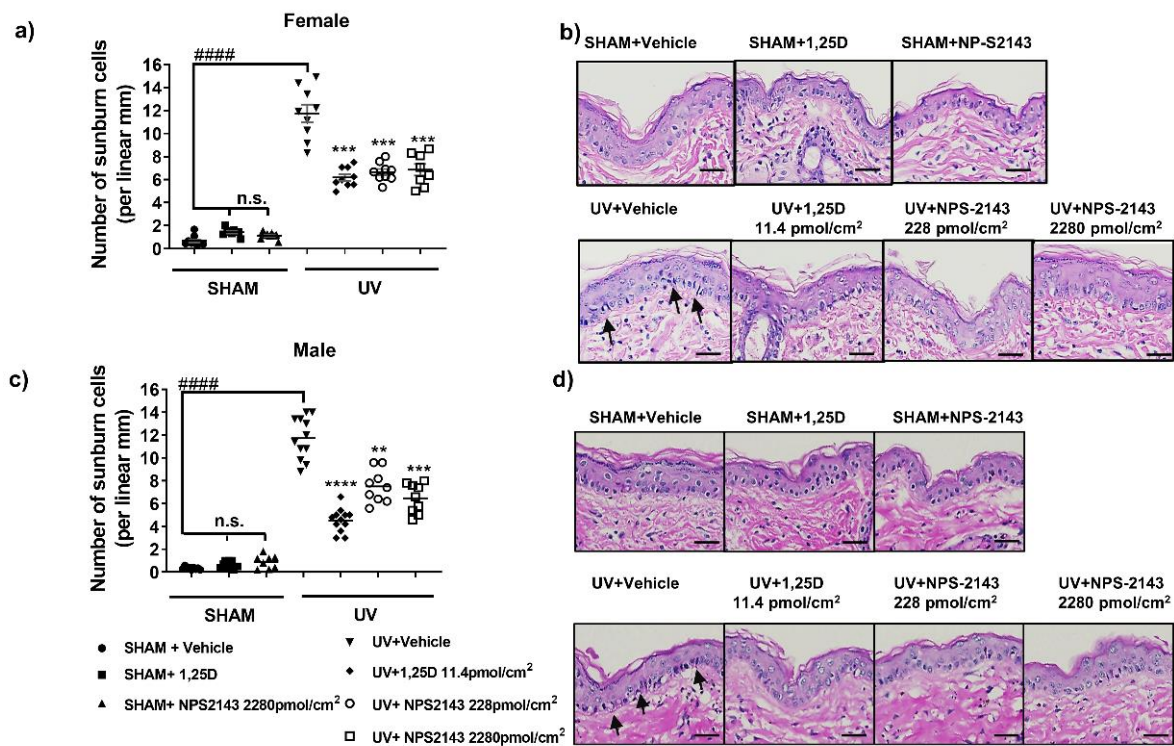


**Figure 2.** NPS-2143 reduces apoptotic keratinocytes in female and male mouse skin following acute UV irradiation. Immediately after exposure to ssUV, female and male Skh:hr1 mice were treated with vehicle 1,25D (11.4 pmol/cm<sup>2</sup>) or NPS-2143 (228 or 2280 pmol/cm<sup>2</sup>) topically, and skin was harvested after 3 h. The number of sunburn cells in female (a) and male (c) mice is presented as displaying data as dot plots. These graphs show representative data from two individual experiments with similar results on each occasion. \*\*\*\*  $p < 0.0001$ , \*\*\*  $p < 0.001$ , \*\*  $p < 0.01$ , and n.s. not significant compared with UV-vehicle treated group by linear mixed model analysis; ####  $p < 0.0001$  significantly different from UV-vehicle by  $t$ -test (a):  $t = 8.417$ ,  $df = 10$  (c):  $t = t = 12.09$ ,  $df = 14$ .  $n = 9$  (triplicate biopsies per mice, 3 mice per group). (b,d) Photomicrographs of UV-induced sunburn cells in female (b) or male (d) mice. Arrows show histological appearance of apoptotic sunburn cells in haematoxylin and eosin stained Skh:hr1 mouse skin section with shrunken, elongated nuclei-stained dark purple. Scale bars = 100  $\mu$ m.

In order to study how UV exposure affects contact hypersensitivity to oxazolone, female mice were exposed to ssUV or SHAM, then treated topically with the various agents. One week later, all the mice were sensitized with 2% oxazolone applied to the non-irradiated abdominal skin. The mice were then challenged one week after this, by topical application of oxazolone to the ears to trigger swelling. Ear thickness measurements were taken before the challenge and again 18 h later. The average ear swelling expressed as the difference between ear thickness measured before and after challenge (at 18 h) in the non-UV exposed (SHAM) vehicle-treated mice was  $293 \pm 45$  microns, and there were no differences among all non-irradiated groups (Figure 3b). In the UV-irradiated vehicle-treated mice, the average ear swelling of vehicle-treated mice was  $155 \pm 30$  microns, indicating significant suppression of the immune response. With topical treatment with 1,25D, average ear swelling after UV was  $217 \pm 52$  microns (Figure 3b), consistent with partial restoration of the contact hypersensitivity response. Though this swelling in response to oxazolone was smaller than in the SHAM with 1,25D-treated mice, the response was significantly better than in the vehicle-treated UV-exposed mice ( $p < 0.05$ ,  $F(3.172, 28.55) = 21.73$ ). Mice treated with NPS-2143 and UV had a measured average ear swelling of  $177 \pm 63$  microns, not significantly different from vehicle-treated, UV exposed mice (Figure 3b). When calculated as a percent immune suppression after UV [31], the values were 52% immune

suppression in the vehicle-treated group, 26% in the 1,25D-treated group ( $p < 0.05$  vs vehicle-treated), and 39% in the mice treated with NPS-2143 (n.s. vs vehicle-treated mice) ( $F(1.582, 21.36) = 3.405$ ) (Figure 3c).

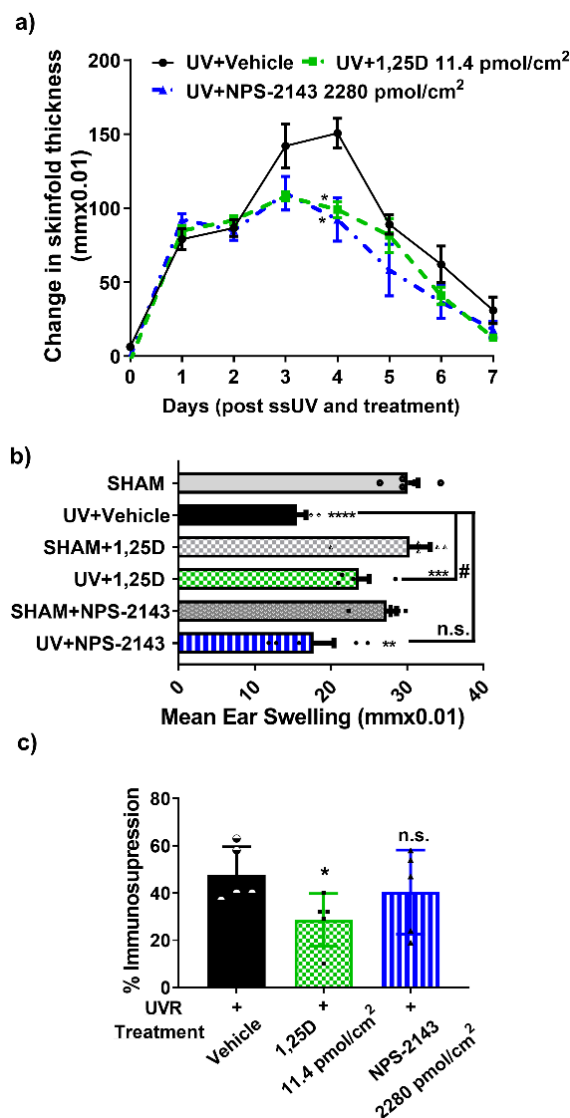


**Figure 3.** The effect of NPS-2143 on ssUV-induced inflammatory edema and the contact hypersensitivity reaction to oxazolone in female Skh:hr1 mice. (a) Measurement of edema daily (days 1–7) by mean change in dorsal skinfold thickness  $\pm$  SEM compared to non-irradiated skinfold thickness. \*  $p < 0.05$  when compared with UV Vehicle treated group.  $n = 5$  mice per group by linear mixed model analysis. (b) Ear Swelling, \*\*\*\*  $p < 0.0001$  \*\*\*  $p < 0.001$ , \*\*  $p < 0.01$  significantly different from SHAM group, #  $p < 0.05$ , n.s. not significant compared with UV-vehicle-treated group, by linear mixed model analysis,  $n = 5$  mice per group. (c) SSUV-induced immunosuppression, \*  $p < 0.05$ , n.s. not significant compared with UV-vehicle-treated group by linear mixed model analysis,  $n = 5$  mice per group.

### 2.3. Study of NPS-2143 in Photocarcinogenesis in Female SKh:hr1 Mice

Albino hairless Skh:hr1 mice develop papillomas and then SCC after 10 weeks of chronic ssUV exposure [31,34,43]. During the 40 weeks of study, tumours normally appeared as small papillomas which gradually increased in diameter (Figure 4a). Papillomas are a benign outgrowth of skin in mice, comparable to the onset of actinic keratoses (AK) in humans [44]. A proportion of these papillomas showed signs of progression towards malignancy. These may be identified grossly and verified histologically as squamous cell carcinomas in later weeks (Figure 4a) [34].

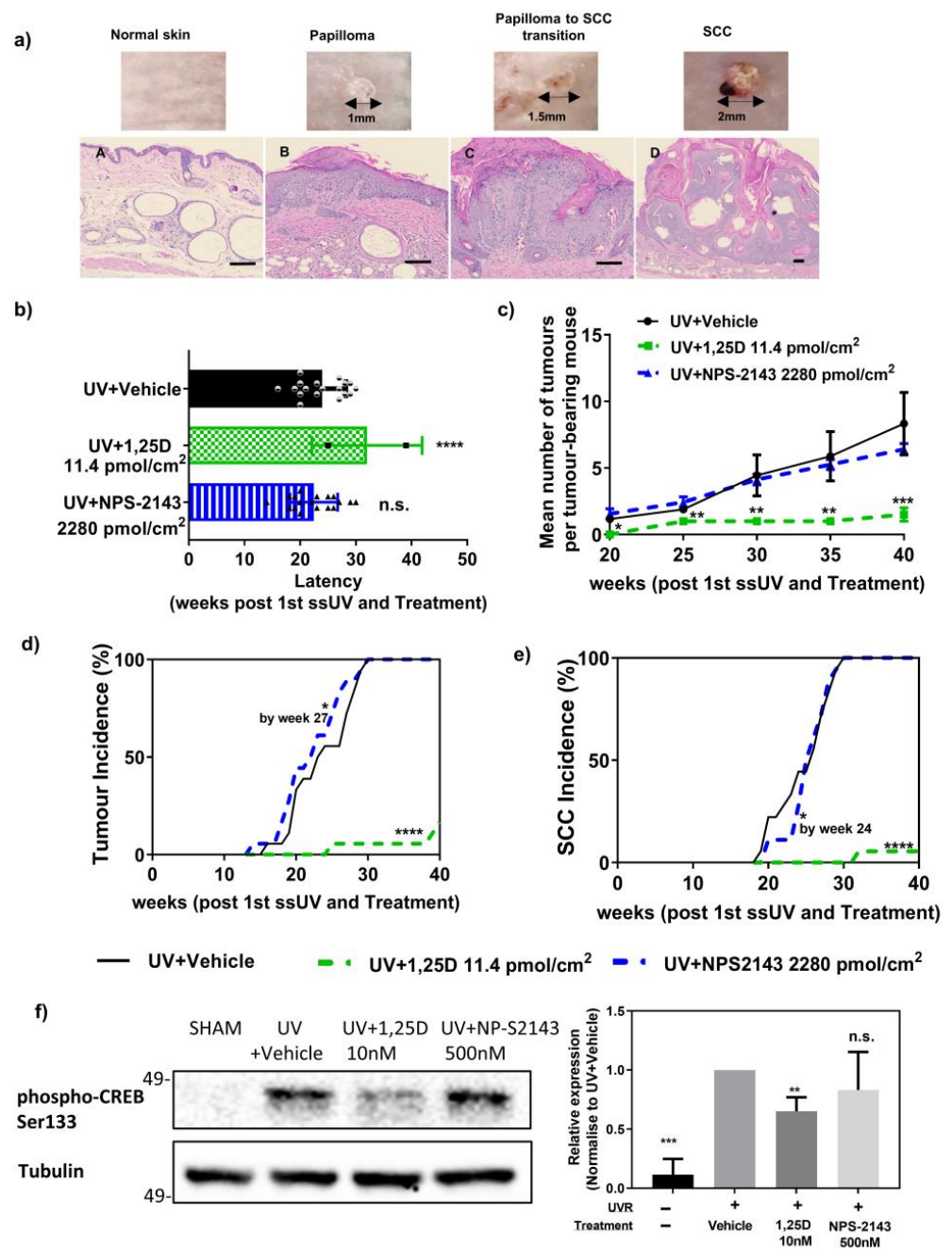


**Figure 4.** Effect of NPS-2143 in chronic SSUV-induced photocarcinogenesis in Skh:hr1 mice. (a) Photographic and photomicrographic examples of (A) normal skin, (B) papilloma, (C) papilloma to SCC transition, and (D) SCC as seen in this study. Scale bar = 100 μm. (b) Tumour Latency (c) Tumour Multiplicity \*\*\*\*  $p < 0.0001$ , \*\*\*  $p < 0.001$ , \*\*  $p < 0.01$ , n.s. not significantly different from UV + Vehicle group. (d) Tumour Incidence (e) SCC incidence \*  $p < 0.05$ , \*\*\*\*  $p < 0.0001$  significantly different from UV + Vehicle group at indicated week by Mantel-Cox test. Each of these graphs illustrates data from a single experiment ( $n = 18$ ) and is presented as means  $\pm$  SEM. (f) Western Blot and densitometry of p-CREB and tubulin (loading control). Human keratinocytes cultured in 96 well plates were irradiated with 400 mJ/cm<sup>2</sup> UVB followed by treatment with vehicle, 10 nM 1,25(OH)<sub>2</sub>D<sub>3</sub> or 500 nM NPS-2143 in the presence of 1 mM CaCl<sub>2</sub> for 90 min. Densitometry of triplicate blots (Figure S1a) for p-CREB expression (Mean + SD) was normalized to UV + Vehicle and shown as a relative expression. Statistical significance was calculated with GraphPad prism using a one-way ANOVA followed by Tukey’s test. \*\* $p < 0.01$ , \*\*\*  $p < 0.001$ , n.s. not significant when compared with vehicle-treated cells after UV.

- **Tumour latency**

The onset of detectable tumour (papilloma) formation in mice varied between treatment groups. As shown in Figure 4b, the latency in the vehicle-treated group was  $24.0 \pm 1.0$  weeks. A significantly increased latency of  $33.6 \pm 2.5$  weeks ( $p < 0.0001$ ,  $F(2, 35) = 2.560$ ) was seen in 1,25D-treated mice ( $11.4 \text{ pmol/cm}^2$ ). The average latency for NPS-2143-treated mice ( $2280 \text{ pmol/cm}^2$ ) was  $22.4 \pm 1.0$  weeks, which was not significantly different from the vehicle control (Figure 4b).

- **Tumour multiplicity**

Tumour multiplicity including both papillomas and SCCs was calculated at each weekly time point, as the average number of tumours per tumour-bearing mouse. Figure 4c shows tumour multiplicity throughout the 40-week study. Vehicle- and NPS-2143 ( $2280 \text{ pmol/cm}^2$ )-treated mice showed a steady increase in tumour multiplicity from week 16 to week 40, while 1,25D-treated mice ( $11.4 \text{ pmol/cm}^2$ ) had remarkably lower tumour multiplicity. Compared to vehicle-treated mice, tumour multiplicity was significantly reduced in the 1,25D-treated group at all week-points assessed ( $p < 0.05$  at week 20,  $p < 0.01$  at week 25, 30 and 35,  $p < 0.005$  at week 40,  $F(2, 45) = 2.255$ ). However, there was no significant difference between NPS-2143 treated and vehicle-treated mice.

- **Tumour incidence**

Progressive total tumour incidence including both papillomas and SCCs was calculated each week as the percentage of mice in each group bearing at least one tumour, as shown in Figure 4d. The incidence data were analysed statistically using a Mantel–Haenszel log-rank test (Mantel–Cox test) [45], in which all treatments were compared to vehicle-treated mice at 27 weeks and after (Table 1a). This analysis reveals whether there was a difference in the risk of developing a tumour. Mice treated with 1,25D ( $11.4 \text{ pmol/cm}^2$ ) had significantly reduced tumour incidence compared with the vehicle-treated group throughout the entire experiment (Figure 4d green dotted line, Table 1a, Mantel–Cox test Chi-square Value = 27.09,  $df = 1$ ). NPS-2143-treated ( $2280 \text{ pmol/cm}^2$ ) mice demonstrated a time point-dependent increase in total tumour incidence compared to the vehicle-treated group at 27 weeks after the first irradiation, but by 28 weeks and over the subsequent period until 40 weeks, there was no significant difference (Figure 4d blue dotted line, Table 1a, Mantel–Cox test Chi-square Value = 4.061,  $df = 1$ ).

**Table 1.** (a) Tumour Incidence and (b) SCC incidence analysed using a Mantel–Cox test.

(a) Total Incidence by Mantel-Haenszel Log Rank Analysis	Significance by Week 27	Significance by Week 28
Vehicle vs. 1,25D $11.4 \text{ pmol/cm}^2$	**** ( $p < 0.0001$ )	**** ( $p < 0.0001$ )
Vehicle vs. NPS-2143 $2280 \text{ pmol/cm}^2$	* ( $p = 0.044$ )	n.s ( $p = 0.21$ )
(b) SCC incidence by Mantel-Haenszel Log Rank Analysis	Significance by week 24	Significance by week 25
Vehicle vs. 1,25D $11.4 \text{ pmol/cm}^2$	**** ( $p < 0.0001$ )	**** ( $p < 0.0001$ )
Vehicle vs. NPS-2143 $2280 \text{ pmol/cm}^2$	* ( $p = 0.02$ )	n.s. ( $p = 0.15$ )

Mice developed squamous cell carcinomas (SCCs) throughout the study from 18 weeks. The SCC-only incidence is shown in Figure 4e. Mice treated with 1,25D ( $11.4 \text{ pmol/cm}^2$ ) had significantly reduced SCC incidence compared with the vehicle control group throughout the experiment (Figure 4e green dotted line, Table 1b, Mantel–Cox test Chi-square Value = 5.355,  $df = 1$ ). Only one mouse in the group of 18 (5.5%) treated with 1,25D developed an SCC at week 32 and this was still present at the end of the study. NPS-2143-treated mice had a significantly lower risk of developing SCC (5 out of 18, 27.8%) compared to the vehicle-treated group (8 out of 18, 44.4%) at the 24th week post-irradiation (Figure 4e Blue

dotted line, Table 1b, Mantel-Cox test Chi-square Value = 22.09, df = 1). However, from the 25th week until the end of the experiment, there was no significant difference between the risk of SCC in NPS-2143- and vehicle-treated mice (Table 1b).

- Phosphorylation of cyclic AMP response element binding protein (CREB) as a predictor of anti-tumour activity

After UV exposure, CREB phosphorylation in epidermal cells increases and this has been proposed as a marker of tumour promoting activity [46]. In this study, 1,25D significantly reduced the risk of developing papillomas and SCC compared with the vehicle-treated group, while NPS-2143 had no overall effect on tumour or SCC incidence (Figure 4e, Table 1b).

Phosphorylation of CREB after UV, 1,25D, or NPS-2143 was studied in normal human keratinocytes. Negligible basal phospho-CREB (p-CREB) was seen in non-irradiated keratinocytes (SHAM) (Figure 4f). In cultured human keratinocytes, exposure to ssUV increased p-CREB measured 90 min after exposure (Figure 4f). Treatment of the cells immediately after UV with 1,25D significantly reduced p-CREB while treatment with NPS-2143 had no effect whether expressed as a function of tubulin as loading control (Figure 4f,  $F(3, 8) = 0.8378$ , and Figure S1a,) or as a function of total CREB (Figure S1b).

A summary of the main differences between responses to the positive control 1,25D and NPS-2143 is shown below (Table 2).

**Table 2.** A schematic representation of the differences between the effects of 1,25D and NPS-2143.

	In Vitro Photoprotection (Yang et al., 2022 [26])	In Vivo Photoprotection against UV-Induced DNA Damage and Sunburn	Protection against UV-Induced Acute Skin Inflammation	Protection against UV-Induced Im- munosuppression	Prevent Skin Carcinogenesis
1,25D	✓	✓	✓	✓	✓
NPS-2143	✓	✓	✓	✗	Delayed initiation but no long-term protection

### 3. Discussion

In this study, the CaSR negative allosteric modifier NPS-2143, like the positive control 1,25D, when applied topically immediately after ssUV, effectively reduced UV-induced DNA lesions of CPD and 8-OHdG in female Skh:hr1 mice. Both NPS-2143 and 1,25D reduced oxidative DNA damage in male mice and at the higher concentration, NPS-2143 also reduced CPD in male mice. These results are consistent with the findings from our study using keratinocytes in primary culture from male human donors [26]. This is a discovery of a photo-protective role for NPS-2143, entirely different from its better recognised role as a therapeutic agent for raising parathyroid hormone levels. NPS-2143 negatively modulates the affinity of the CaSR for extracellular  $Ca^{2+}$ , thereby reducing its activity [21–25]. In order to better discriminate the role of the CaSR in this study, it would have been useful to examine a CaSR antagonist (NPS2390 or Calcium-Sensing Receptor Antagonists I), but these studies were beyond the resources available for this work.

Sunburn cells and apoptotic keratinocytes were observed as soon as 3 h after acute exposure to UVB [47], despite being cells that undergo programmed cell death as a result of extensive and irreparable DNA damage [42]. It is reasonable to propose that reduced DNA damage, along with increased DNA repair [21] in the presence of NPS-2143, led to fewer apoptotic keratinocytes in mouse skin. In the meantime, we also observed improved survival of human keratinocytes in culture after UV exposure in the presence of NPS-2143 (Figure S2). It is likely that reduced generation of ROS, as previously reported with NPS-2143 after UV [21], contributed to reduced apoptosis. While sunburn cells are an index of apoptosis, analysis of more specific markers of apoptosis such as caspase3/7 or cleaved

PARP in the mouse tissue would indicate early stages of apoptotic events and could help to elucidate the mechanism.

The reductions in 8-OHdG in male mice with 1,25D or NPS-2143 were similar to those seen in female mice. However, only the higher dose of NPS-2143 reduced CPD in male mice. Resistance in male mice to protection against UV-induced CPD in the presence of 1,25D has been previously reported in a separate study [47]. In that study, we demonstrated that the estrogen receptor- $\beta$  (ER- $\beta$ ), the only estrogen receptor present in female mouse skin, seemed likely to be involved in reductions in CPD with 1,25D, since treatment with an ER- $\beta$  antagonist or the use of female ER- $\beta$  knockout mice reduced the response to 1,25D [47]. The current results indicate less effective protection against UV-induced CPD by a negative allosteric modulator of the CaSR. Whether this is also related to the presence of ER- $\beta$  in female mouse skin or some other sex-related difference is an interesting question but was beyond the scope of the current study. A simple explanation for the reduced effectiveness of the lower dose of NPS-2143 could be that male mice have approximately 20% thicker skin than female mice, regardless of UV [48]. DNA damage is a major contributor to UV-induced immune suppression [49] and susceptibility of male mice or humans to UV-induced immune suppression is greater than in their female counterparts [50,51]. Male mice are more susceptible than females to photocarcinogenesis [52], whereas incidence and mortality of skin cancers is greater in men [53,54].

Given resource limitations, the increased potential for male mice to fight and scratch, producing skin damage which would interfere with observations [55], meant that longer studies of skin edema, immune suppression, and tumour development after UV were only undertaken in female mice.

Topical NPS-2143, like 1,25D, produced a significant decrease in skin edema of mice, reflecting reduced inflammation after ssUV. UVR induces immediate and sustained production in NO in the skin [56–59] promoting the secretion of inflammatory mediators such as IL-6 [60]. A major limitation of the study is that it was not possible under the circumstances to examine a cytokine profile of mouse skin tissue before and after UV with or without NPS-2143 or 1,25D. Nevertheless, from the literature, there is evidence that NPS-2143 reduces NLRP3 inflammasome activation [61–63], overproduction of NO [64,65], the pro-inflammatory cytokine IL-6, and more [66–69]. These observations could explain the ability of NPS-2143 to reduce inflammation in mouse skin on day four after UV.

Somewhat surprisingly, despite a reduction in skin inflammation after UV, treatment with NPS-2143 had no effect on UV-induced immune suppression. Both DNA damage and increased IL-6 are important promoters of UV-dependent immune suppression [70]. Yet NPS-2143, like 1,25D, reduced DNA damage and, from the literature, also reduces IL-6 [66–69]. UV can directly damage antigen-presenting cells and promote the production of immunosuppressive cytokines such as IL-10 and IL-4 [71–73]. IL-10 is an anti-inflammatory cytokine and a potent immunosuppressant [74]. Secreted by UV-irradiated keratinocytes [75,76] and regulatory T cells [77], IL-10 not only prevents T cell expansion and activation but can also suppress other antigen-presenting cells [74]. It has been shown that reductions in CPD using liposomes containing T4N5 endonuclease led to reduced UV-immune suppression due to decreases in UV-upregulated IL-10 and TNF- $\alpha$  at both the mRNA and protein levels [78]. Furthermore, IL-10<sup>-/-</sup> mice were protected against photocarcinogenesis [79]. Though not tested in this study, IL-10 was increased with NPS-2143 treatment in rats [66,69]. This may explain why NPS-2143 failed to prevent UV-induced immunosuppression, though it protected against CPD and inflammation.

Skin tumour development depends on a combination of DNA damage, inflammation, and immunosuppression [49,80]. CPD are a major contributor to UV-induced mutations, so reduced CPDs might lead to fewer UV-induced mutations [80] and thus fewer tumours. Furthermore, enhanced repair of CPDs has been shown to reduce skin cancer incidence in mice [81] and humans [82] and we previously found that NPS-2143 increased DNA repair in keratinocytes [26]. Based on these findings, it seemed possible that NPS-2143 would have some protective capacity at an early stage of photocarcinogenesis due to its ability

to reduce DNA damage and inflammatory reactions *in vivo*. In the photocarcinogenesis study, however, a single concentration of NPS-2143 (2280 pmol/cm<sup>2</sup>) was not superior to vehicle, either in time to develop the first tumour (including benign papilloma) or in the total number of tumours per mouse. Although NPS-2143 significantly reduced SCC incidence at 24 weeks, the effect did not persist.

Although the failure of NPS-2143 to prevent UV-induced immune suppression may explain its failure to prevent tumours in the chronic UV study, other factors may be involved. Cyclic AMP Response Element Binding protein (CREB) is a transcription factor essential for basic cellular function and homeostasis [83]. CREB is activated by phosphorylation at Ser133 by various kinases [83,84]. CREB overexpression supports growth and progression in various cancers [85–89]. CREB activation promotes enhanced cell proliferation, dysregulation of differentiation and reduced sensitivity to apoptosis and metastasis, particularly in melanoma [87,90] and SCC [88,91]. Using human keratinocytes, we observed that UV exposure increased phosphorylation of CREB at Ser 133 (phospho-CREB Ser<sup>133</sup>). While it would have been useful to verify the CREB and p-CREB changes in mouse skin, this was beyond the scope of the study and is a limitation. Our results in human keratinocytes are consistent with a recent study using reverse phase protein microarray analysis, which reported that p-CREB Ser<sup>133</sup> was significantly activated at 1 h, 5 h, and 24 h after a single acute dose of 2MED UV in human skin [92] and with the report of increased p-CREB in mouse skin [46].

It has been argued that p-CREB is important in the initiation of papilloma formation, while other transcription factors such as CCAAT/enhancer binding protein (C/EBP)–B [93,94] control later stages of tumour growth and Activator Protein 1 (AP1) [95–97] maintains tumour identity. In a study of SCC, shRNA-mediated knockdown of CREB resulted in a significant increase in G2 phase arrest and a reduction in tumorigenic activity [91]. These authors identified that a key transcription factor complex, CREB and RFX1, which binds in the nucleus and is stabilized by CCAR2, is required to maintain proliferation in SCC [91]. Overexpression of CREB in a human squamous carcinoma cell line SCC13 remarkably increased its colony forming ability via a  $\beta$ -catenin-dependent pathway [88]. These studies suggest critical functions of CREB not only in the initial stage of papilloma formation but also in the development of neoplastic characteristics of SCC. Treatment of keratinocytes with 1,25D reduced UV-induced expression of p-CREB, fitting with its ability to protect mouse skin from developing both papillomas and SCC in the photocarcinogenesis study. NPS-2143, on the other hand, did not reduce UV-upregulated p-CREB. This may be part of the explanation for its inability to reduce tumour incidence, apart from its failure to decrease UV-induced immunosuppression.

Bikle et.al reported that double knockout of the vitamin D receptor and CaSR in the epidermis leads to spontaneous SCC formation in mice without any induction by UV, which was not observed in mice with deletion of either gene alone [98,99]. Those studies did not involve UV exposure. This is the first study to investigate whether negative modulation of the CaSR in skin alters responses to UV. NPS-2143 reduced two types of DNA damage in epidermal cells as well as skin inflammation to a similar extent as 1,25D, a known photo-protective agent (Figures 1–3). However, NPS-2143 did not ameliorate UV-induced immune suppression (Figure 3). This latter observation, together with the failure of NPS-2143 to reduce post-UV CREB phosphorylation, probably explain the limited effect of this compound on skin tumour formation after ssUV (Figure 4). It is possible that the reduction in UV-induced DNA damage including oxidative damage by NPS-2143 may indicate an anti-aging effect [100]. These novel findings may lead to new research directions on the relationship between UV and the CaSR.

## 4. Materials and Methods

### 4.1. Studies in Mice

The *in vivo* studies were approved by the Animal Ethics Committee of the University of Sydney (Approval number: 2015/794) and conformed to ARRIVE criteria. Skh:hr1

hairless albino mice, originally from Charles River (Wilmington, MA, USA), were from an in-house colony maintained at the University of Sydney. All Skh:hr1 hairless mice were housed in groups in wire-topped plastic boxes at an ambient temperature of 23–25°C under gold lighting (F40GO tubes, General Electric Co., Hobart, TAS, Australia) that does not emit UV radiation, and fed with Gordon Rat and Mouse Pellets (Yanderra, NSW, Australia) and tap water ad libitum. Male and female Skh:hr1 mice that were aged-matched in groups were used for experiments [31]. Mice were not allowed to be housed singly for this study but were housed in groups. Female mice are less prone to fighting than male mice and the fighting produces skin damage and artefacts [55]. For this reason, it is possible to study both female and male mice for DNA damage within hours after a UV exposure; however, the use of female mice for studies of skin edema or contact hypersensitivity conducted over 7 days and 16 days, respectively, or photocarcinogenesis (over 40 weeks) is preferred (Figure 5).

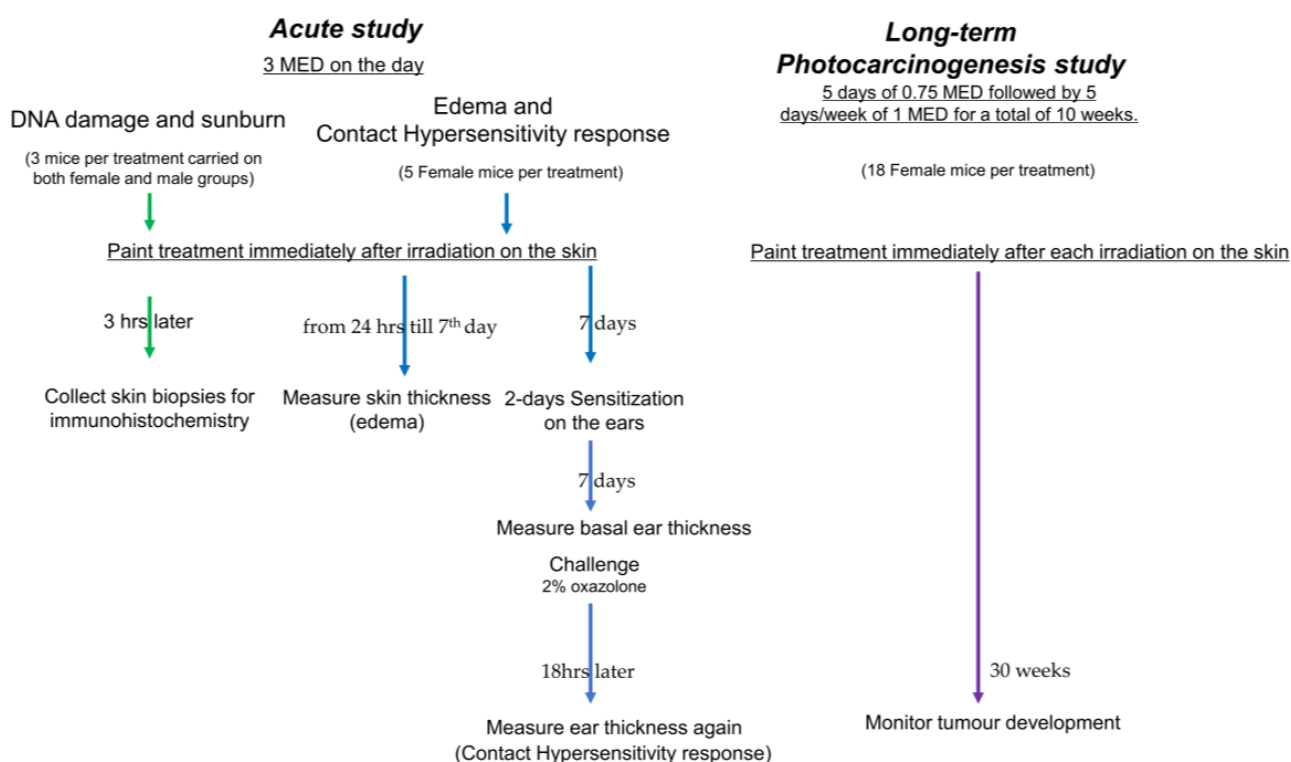


**Figure 5.** Experimental design scheme.

As previously established, the minimum erythemal dose (MED) of UV with this source for Skh:hr1 mice was 1.33 kJ/m<sup>2</sup> UVB and 23.7 kJ/m<sup>2</sup> UVA [31,101]. UV-irradiated mice were subjected to a single dose of 3 MED of UV (UVB value at 3.99 kJ/m<sup>2</sup>) for acute and immunosuppression studies. In the chronic photocarcinogenesis study, mice were subjected to 5 days of 0.75 MED followed by 5 days/week of 1 MED, for a total of 10 weeks (Figure 5).

#### 4.2. Topical Treatments, DNA Damage and Sunburn Cells

Mice were treated topically over approximately 7 cm<sup>2</sup> on the irradiated dorsal skin with 100 µL of vehicle only, or vehicle containing 1,25D (Sapphire Bioscience Pty Ltd., Redfern, NSW, Australia), or NPS-2143 2143 (HY-1007 MCE<sup>®</sup>, Medchem Express, Monmouth Junction, NJ, USA) immediately after irradiation, as previously described [31]. The compounds (1,25D and NPS-2143) were freshly diluted in spectroscopic grade ethanol (Merck, Darmstadt, Germany), combined with propylene glycol (Sigma-Aldrich, St. Louis, MO, USA) and MilliQ water at a ratio of 2:1:1 (v/v/v). Vehicle (base lotion) was combined, ethanol:propylene glycol:water 2:1:1 v/v [31]. The dose of NPS-2143, equivalent to 20×

(228 pmol/cm<sup>2</sup>) and 200× (2280 pmol/cm<sup>2</sup>) of an effective dose of 1,25D 11.4 pmol/cm<sup>2</sup> was determined according to the same ratio of 1,25D doses as determined from in vitro experiments [26,31]. Biopsies of dorsal skin were taken in triplicate from each mouse, 3 h post-UV and paraffin-embedded for immunohistochemistry of DNA damage as previously described [31]. Quantification of positive nuclei as % total nuclei (the percentage of CPD or 8-OHd positive nuclei staining in the selected nuclei in an area of epidermis) was obtained using MetaMorph (Molecular Devices, San Jose, CA, USA) and normalized to SHAM.

Routine haematoxylin and eosin staining was carried out by Veterinary Pathology Diagnostic Service (University of Sydney) to visualize sunburn cells. The stained sections were examined under a Zeiss Axioscan light microscope (Oberkochen, Germany) at 20× magnification, and the number of sunburn cells per linear millimetre of skin section recorded, as previously described [31,47]. Non-irradiated samples as SHAM control were obtained from the abdomen. Three areas of each section were analysed.

#### 4.3. Skin Edema and Induction of Contact Hypersensitivity in Mice

Changes in dorsal skin thickness, a measure of edema, were recorded daily from 24 h onward until the levels returned close to pre-UV condition on the 7th day after irradiation.

The contact hypersensitivity response was tested to investigate the effects of NPS-2143 on UV-induced systemic immunosuppression, as previously described [31]. Briefly, female mice were sensitized 1 week after irradiation and treatments, with 100 µL of 2% oxazolone (Sigma-Aldrich, USA) (*w/v*) in absolute alcohol applied to the non-irradiated abdominal skin. Sensitization was repeated on the subsequent day. The sensitized mice were challenged 2 weeks after irradiation by application of 5 µL 2% oxazolone to both surfaces of each ear, so that each mouse received 20 µL in total. Ear thickness measurements, taken using a spring micrometre (Interapid, Zurich, Switzerland), were recorded before the challenge and at 18 h after challenge, as previously reported [31]. The difference between pre- and post-oxazolone challenge ear thickness measurements of each mouse was recorded as ear swelling and the means for each group of 5 mice was calculated. Ear Swelling = pre-challenge ear thickness – post-challenge ear thickness.

The immune response was then calculated for each mouse, as shown in the formula below:

$$\text{Immune Response} = \frac{\text{Ear swelling of UV IRRADIATED mice}}{\text{Ear swelling of UV NON – IRRADIATED (SHAM) mice}} \quad (1)$$

Immunosuppression was calculated as 100% minus this value, ± SEM [31] as in the formula below:

$$\text{Immunosuppression \%} = (1 - \text{Immune Response}) \times 100 \quad (2)$$

#### 4.4. Photocarcinogenesis

For this study, groups of 18 mice were used. Immediately after ssUV irradiation, mice were treated topically with either base lotion [31], 1,25D (11.4 pmol/cm<sup>2</sup>), or NPS-2143 (2280 pmol/cm<sup>2</sup>). During the next 30 weeks, the time of appearance, location, and visual identification of tumours with a diameter of at least 1 mm were monitored and mapped for each mouse. As previously described [31], the term “tumour” includes papilloma and SCC. The photocarcinogenic outcomes were reported as tumour latency, tumour incidence, tumour multiplicity, and SCC incidence. At the end of the experiment, all tumours were harvested for histological examination to confirm the classification.

#### 4.5. Culture of Primary Human Keratinocytes

Keratinocytes were harvested from skin samples under University of Sydney Human Research Ethics Committee protocol no. 2015/063 and cultured, as previously described [26]. The concentration of NPS-2143 used in these in vitro studies was based on previous experiments where we performed serial dilutions of NPS-2143 to determine the

concentration-dependent response in human keratinocytes [26]. A total of 500 nM was in the effective concentration range (5 nM~500 nM) and was also  $10\times$  IC 50; thus, it was chosen for all the in vitro experiments.

#### 4.6. Western Blot

Keratinocytes were irradiated with an Oriel 1000 W xenon arc lamp (Newport Corporation, USA) and subsequently treated with vehicle, 1,25D, or NPS-2143, as in our previous study [26]. Western blot was performed, as previously described [102], with  $\alpha$ -tubulin as the loading control. Primary antibodies used in this study were anti-phospho-CREB (Ser133) at 1 in 1000 dilution (mouse monoclonal, #9196, Cell Signaling Technology, Trask Lane Danvers, MA, USA), anti-CREB(Total) at 1 in 1000 dilution (mouse monoclonal, #9197, Cell Signaling Technology, Trask Lane Danvers, MA, USA), or anti-tubulin at 1  $\mu$ g/mL (mouse monoclonal, SC-5286, Santa Cruz Biotechnology). The band was imaged with the ChemiDoc<sup>TM</sup> imaging system (Bio-Rad Laboratories, Inc, Hercules, CA, USA) and densitometry was carried out using Image J. SHAM, showing negligible expression of p-CREB which served as a negative control, and the data was normalized to UV+ vehicle to pool experiments.

#### 4.7. Statistical Analysis

Animals in this study were divided into treatment groups of three for acute study, groups of five for immunosuppression study, and groups of eighteen for chronic photocarcinogenesis [31,47,101,103]. These numbers were determined by power analysis manually calculated from data from previous studies to have an 80% chance showing a 20% difference between treatment group at a significance level of 5% [104,105]. Results are expressed as either as mean + SEM or as indicated. All the data sets passed goodness of fit tests, which determine whether sample data exhibit skewness and kurtosis that matches a normal distribution. All statistical analyses were performed with GraphPad Prism statistical program 9.0 (GraphPad Software Inc.). Unless otherwise stated, analysis of comparisons between treatment groups were made by linear mixed-model analysis, appropriate for dealing with repeated measurement data. The Mantel–Haenszel log-rank test (also called Mantel–Cox test) was used to analyse incidence data in the photocarcinogenesis study [31,45].

**Supplementary Materials:** The following supporting information can be downloaded at: <https://www.mdpi.com/article/10.3390/ijms24054921/s1>.

**Author Contributions:** Conceptualization: C.Y., R.S.M., A.D.C. and M.S.R.; Data curation: C.Y. and M.S.R.; Formal analysis: C.Y., J.M. and M.S.R.; Funding acquisition: R.S.M.; Investigation: C.Y., M.S.R. and W.G.M.D.S.; Methodology: M.S.R., C.Y., K.M.D., A.D.C. and R.S.M.; Project Administration: C.Y., M.S.R. and R.S.M.; Resources: A.J.A.H.; Supervision: R.S.M., M.S.R. and A.D.C.; Validation: M.S.R., J.M. and A.D.C.; Visualization: C.Y. and M.S.R.; Writing—original draft: C.Y.; Writing—review and editing: R.S.M., M.S.R., A.D.C., A.J.A.H., J.M., K.M.D. and W.G.M.D.S. All authors have read and agreed to the published version of the manuscript.

**Funding:** This research was funded by National Health and Medical Research Council APP1070688.

**Institutional Review Board Statement:** All studies of human tissue were approved by the Human Research Ethics Committee of the University of Sydney (protocol no. 2015/063). The studies in mice were approved by the Animal Ethics Committee of the University of Sydney (protocol no. 2015/794).

**Informed Consent Statement:** Informed consent was obtained from all subjects or parents/guardians involved in the study for collection of skin tissue and publication of results. Skin tissue samples were de-identified after collection.

**Data Availability Statement:** The data that support the findings of this study are available from the corresponding author upon reasonable request. Some data may not be made available because of privacy or ethical restrictions.

**Acknowledgments:** Alex Shaw and Stanislaus Stadlmann from the Sydney Informatics Hub, University of Sydney are thanked for additional statistical help.

**Conflicts of Interest:** The authors declare no conflict of interest.

## References

1. Douki, T.; Bretonniere, Y.; Cadet, J. Protection against radiation-induced degradation of DNA bases by polyamines. *Radiat. Res.* **2000**, *153*, 29–35. [[CrossRef](#)] [[PubMed](#)]
2. Cooke, M.S.; Podmore, I.D.; Mistry, N.; Evans, M.D.; Herbert, K.E.; Griffiths, H.R.; Lunec, J. Immunochemical detection of UV-induced DNA damage and repair. *J. Immunol. Methods* **2003**, *280*, 125–133. [[CrossRef](#)]
3. Mouret, S.; Charveron, M.; Favier, A.; Cadet, J.; Douki, T. Differential repair of UVB-induced cyclobutane pyrimidine dimers in cultured human skin cells and whole human skin. *DNA Repair* **2008**, *7*, 704–712. [[CrossRef](#)] [[PubMed](#)]
4. Ikehata, H.; Ono, T. Significance of CpG methylation for solar UV-induced mutagenesis and carcinogenesis in skin. *Photochem. Photobiol.* **2007**, *83*, 196–204. [[CrossRef](#)]
5. Hruza, L.L.; Pentland, A.P. Mechanisms of UV-induced inflammation. *J. Investig. Dermatol.* **1993**, *100*, 35S–41S. [[CrossRef](#)]
6. Halliday, G.M. Inflammation, gene mutation and photoimmunosuppression in response to UVR-induced oxidative damage contributes to photocarcinogenesis. *Mutat. Res.* **2005**, *571*, 107–120. [[CrossRef](#)] [[PubMed](#)]
7. Hart, P.H.; Norval, M. Ultraviolet radiation-induced immunosuppression and its relevance for skin carcinogenesis. *Photochem. Photobiol. Sci.* **2018**, *17*, 1872–1884. [[CrossRef](#)]
8. Ananthaswamy, H.N. Ultraviolet Light as a Carcinogen. In *Comprehensive Toxicology, Chemical Carcinogens and Anticarcinogens*; Bowden, G.T., Fischer, S.M., Eds.; Pergamon: Oxford, UK, 1997; Volume 12.
9. Peak, M.J.; Peak, J.G.; Carnes, B.A. Induction of direct and indirect single-strand breaks in human cell DNA by far- and near-ultraviolet radiations: Action spectrum and mechanisms. *Photochem. Photobiol.* **1987**, *45*, 381–387. [[CrossRef](#)]
10. Kripke, M.L.; Fisher, M.S. Immunologic parameters of ultraviolet carcinogenesis. *J. Natl. Cancer Inst.* **1976**, *57*, 211–215. [[CrossRef](#)]
11. Rangwala, S.; Tsai, K.Y. Roles of the immune system in skin cancer. *Br. J. Dermatol.* **2011**, *165*, 953–965. [[CrossRef](#)]
12. Katiyar, S.K. UV-induced immune suppression and photocarcinogenesis: Chemoprevention by dietary botanical agents. *Cancer Lett.* **2007**, *255*, 1–11. [[CrossRef](#)]
13. Scott, T.L.; Christian, P.A.; Kesler, M.V.; Donohue, K.M.; Shelton, B.; Wakamatsu, K.; Ito, S.; D’Orazio, J. Pigment-independent cAMP-mediated epidermal thickening protects against cutaneous UV injury by keratinocyte proliferation. *Exp. Dermatol.* **2012**, *21*, 771–777. [[CrossRef](#)]
14. de Winter, S.; Vink, A.A.; Roza, L.; Pavel, S. Solar-simulated skin adaptation and its effect on subsequent UV-induced epidermal DNA damage. *J. Investig. Dermatol.* **2001**, *117*, 678–682. [[CrossRef](#)] [[PubMed](#)]
15. Young, A.R.; Potten, C.S.; Chadwick, C.A.; Murphy, G.M.; Hawk, J.L.; Cohen, A.J. Photoprotection and 5-MOP photochemoprotection from UVR-induced DNA damage in humans: The role of skin type. *J. Investig. Dermatol.* **1991**, *97*, 942–948. [[CrossRef](#)]
16. Gniadecka, M.; Wulf, H.C.; Mortensen, N.N.; Poulsen, T. Photoprotection in vitiligo and normal skin—A quantitative assessment of the role of stratum corneum, viable epidermis and pigmentation. *Acta Derm.-Venereol.* **1996**, *76*, 429–432.
17. Bikle, D.D.; Xie, Z.; Tu, C.L. Calcium regulation of keratinocyte differentiation. *Expert Rev. Endocrinol. Metab.* **2012**, *7*, 461–472. [[CrossRef](#)]
18. Tu, C.L.; Crumrine, D.A.; Man, M.Q.; Chang, W.; Elalieh, H.; You, M.; Elias, P.M.; Bikle, D.D. Ablation of the calcium-sensing receptor in keratinocytes impairs epidermal differentiation and barrier function. *J. Investig. Dermatol.* **2012**, *132*, 2350–2359. [[CrossRef](#)]
19. Bikle, D.D.; Ratnam, A.; Mauro, T.; Harris, J.; Pillai, S. Changes in calcium responsiveness and handling during keratinocyte differentiation. Potential role of the calcium receptor. *J. Clin. Investig.* **1996**, *97*, 1085–1093. [[CrossRef](#)] [[PubMed](#)]
20. Tu, C.L.; Chang, W.; Bikle, D.D. The extracellular calcium-sensing receptor is required for calcium-induced differentiation in human keratinocytes. *J. Biol. Chem.* **2001**, *276*, 41079–41085. [[CrossRef](#)] [[PubMed](#)]
21. Nemeth, E.F. The search for calcium receptor antagonists (calcilytics). *J. Mol. Endocrinol.* **2002**, *29*, 15–21. [[CrossRef](#)]
22. Nemeth, E.F.; Delmar, E.G.; Heaton, W.L.; Miller, M.A.; Lambert, L.D.; Conklin, R.L.; Gowen, M.; Gleason, J.G.; Bhatnagar, P.K.; Fox, J. Calcilytic compounds: Potent and selective Ca<sup>2+</sup> receptor antagonists that stimulate secretion of parathyroid hormone. *J. Pharmacol. Exp. Ther.* **2001**, *299*, 323–331.
23. Hannan, F.M.; Walls, G.V.; Babinsky, V.N.; Nesbit, M.A.; Kallay, E.; Hough, T.A.; Fraser, W.D.; Cox, R.D.; Hu, J.; Spiegel, A.M.; et al. The Calcilytic Agent NPS 2143 Rectifies Hypocalcemia in a Mouse Model With an Activating Calcium-Sensing Receptor (CaSR) Mutation: Relevance to Autosomal Dominant Hypocalcemia Type 1 (ADH1). *Endocrinology* **2015**, *156*, 3114–3121. [[CrossRef](#)] [[PubMed](#)]
24. Leach, K.; Wen, A.; Cook, A.E.; Sexton, P.M.; Conigrave, A.D.; Christopoulos, A. Impact of clinically relevant mutations on the pharmacoregulation and signaling bias of the calcium-sensing receptor by positive and negative allosteric modulators. *Endocrinology* **2013**, *154*, 1105–1116. [[CrossRef](#)] [[PubMed](#)]
25. Gregory, K.J.; Kufareva, I.; Keller, A.N.; Khajehali, E.; Mun, H.C.; Goolam, M.A.; Mason, R.S.; Capuano, B.; Conigrave, A.D.; Christopoulos, A.; et al. Dual Action Calcium-Sensing Receptor Modulator Unmasks Novel Mode-Switching Mechanism. *ACS Pharmacol. Transl. Sci.* **2018**, *1*, 96–109. [[CrossRef](#)]
26. Yang, C.; Rybchyn, M.S.; De Silva, W.G.M.; Matthews, J.; Holland, A.J.A.; Conigrave, A.D.; Mason, R.S. UV-induced DNA Damage in Skin is Reduced by CaSR Inhibition. *Photochem. Photobiol.* **2022**, *98*, 1157–1166. [[CrossRef](#)] [[PubMed](#)]
27. Nishigori, C. Current concept of photocarcinogenesis. *Photochem. Photobiol. Sci.* **2015**, *14*, 1713–1721. [[CrossRef](#)] [[PubMed](#)]

28. Dixon, K.M.; Deo, S.S.; Wong, G.; Slater, M.; Norman, A.W.; Bishop, J.E.; Posner, G.H.; Ishizuka, S.; Halliday, G.M.; Reeve, V.E.; et al. Skin cancer prevention: A possible role of 1,25-dihydroxyvitamin D<sub>3</sub> and its analogs. *J. Steroid Biochem.* **2005**, *97*, 137–143. [[CrossRef](#)] [[PubMed](#)]
29. Wong, G.; Gupta, R.; Dixon, K.M.; Deo, S.S.; Choong, S.M.; Halliday, G.M.; Bishop, J.E.; Ishizuka, S.; Norman, A.W.; Posner, G.H.; et al. 1,25-Dihydroxyvitamin D and three low-calcemic analogs decrease UV-induced DNA damage via the rapid response pathway. *J. Steroid Biochem. Mol. Biol.* **2004**, *89–90*, 567–570. [[CrossRef](#)] [[PubMed](#)]
30. Dixon, K.M.; Deo, S.S.; Norman, A.W.; Bishop, J.E.; Halliday, G.M.; Reeve, V.E.; Mason, R.S. In vivo relevance for photoprotection by the vitamin D rapid response pathway. *J. Steroid Biochem. Mol. Biol.* **2007**, *103*, 451–456. [[CrossRef](#)] [[PubMed](#)]
31. Dixon, K.M.; Norman, A.W.; Sequeira, V.B.; Mohan, R.; Rybchyn, M.S.; Reeve, V.E.; Halliday, G.M.; Mason, R.S. 1 alpha,25(OH)(2)-Vitamin D and a Nongenomic Vitamin D Analogue Inhibit Ultraviolet Radiation-Induced Skin Carcinogenesis. *Cancer Prev. Res.* **2011**, *4*, 1485–1494. [[CrossRef](#)]
32. Chida, K.; Hashiba, H.; Fukushima, M.; Suda, T.; Kuroki, T. Inhibition of tumor promotion in mouse skin by 1 alpha,25-dihydroxyvitamin D<sub>3</sub>. *Cancer Res.* **1985**, *45*, 5426–5430.
33. Forbes, P.D.; Blum, H.F.; Davies, R.E. Photocarcinogenesis in hairless mice: Dose-response and the influence of dose-delivery. *Photochem. Photobiol.* **1981**, *34*, 361–365. [[CrossRef](#)] [[PubMed](#)]
34. Reeve, V.E.; Ley, R.D. Animal models of ultraviolet radiation-induced skin cancer. In *Prevention of Skin Cancer*; Hill, D., Elwood, J.M., English, D.R., Eds.; Springer: Dordrecht, The Netherlands, 2004; pp. 177–194. [[CrossRef](#)]
35. Brown, K.; Balmain, A. Transgenic mice and squamous multistage skin carcinogenesis. *Cancer Metastasis Rev.* **1995**, *14*, 113–124. [[CrossRef](#)] [[PubMed](#)]
36. Demetriou, S.K.; Ona-Vu, K.; Teichert, A.E.; Cleaver, J.E.; Bikle, D.D.; Oh, D.H. Vitamin D receptor mediates DNA repair and is UV inducible in intact epidermis but not in cultured keratinocytes. *J. Investig. Dermatol.* **2012**, *132*, 2097–2100. [[CrossRef](#)]
37. Mason, R.; Holliday, C.J. 1,25-Dihydroxyvitamin D Contributes to Photoprotection in Skin Cells. In *Vitamin D Endocrine System: Structural, Biological, Genetic and Clinical Aspects*; Norman, A.W., Bouillon, R., Thomasset, M., Eds.; University of California: Riverside, CA, USA, 2000; pp. 605–608.
38. Gupta, R.; Dixon, K.M.; Deo, S.S.; Holliday, C.J.; Slater, M.; Halliday, G.M.; Reeve, V.E.; Mason, R.S. Photoprotection by 1,25 dihydroxyvitamin D<sub>3</sub> is associated with an increase in p53 and a decrease in nitric oxide products. *J. Investig. Dermatol.* **2007**, *127*, 707–715. [[CrossRef](#)] [[PubMed](#)]
39. De Haes, P.; Garmyn, M.; Verstuyf, A.; De Clercq, P.; Vandewalle, M.; Degreef, H.; Vantieghem, K.; Bouillon, R.; Segaert, S. 1,25-Dihydroxyvitamin D<sub>3</sub> and analogues protect primary human keratinocytes against UVB-induced DNA damage. *J. Photochem. Photobiol. B Biol.* **2005**, *78*, 141–148. [[CrossRef](#)]
40. Lee, J.; Youn, J.I. The photoprotective effect of 1,25-dihydroxyvitamin D<sub>3</sub> on ultraviolet light B-induced damage in keratinocyte and its mechanism of action. *J. Dermatol. Sci.* **1998**, *18*, 11–18. [[CrossRef](#)]
41. Manggau, M.; Kim, D.S.; Ruwisch, L.; Vogler, R.; Korting, H.C.; Schafer-Korting, M.; Kleuser, B. 1Alpha,25-dihydroxyvitamin D<sub>3</sub> protects human keratinocytes from apoptosis by the formation of sphingosine-1-phosphate. *J. Investig. Dermatol.* **2001**, *117*, 1241–1249. [[CrossRef](#)]
42. Sheehan, J.M.; Young, A.R. The sunburn cell revisited: An update on mechanistic aspects. *Photochem. Photobiol. Sci.* **2002**, *1*, 365–377. [[CrossRef](#)] [[PubMed](#)]
43. Saran, A.; Spinola, M.; Pazzaglia, S.; Peissel, B.; Tiveron, C.; Tatangelo, L.; Mancuso, M.; Covelli, V.; Giovannelli, L.; Pitozzi, V.; et al. Loss of tyrosinase activity confers increased skin tumor susceptibility in mice. *Oncogene* **2004**, *23*, 4130–4135. [[CrossRef](#)] [[PubMed](#)]
44. Ortonne, J.P. From actinic keratosis to squamous cell carcinoma. *Br. J. Dermatol.* **2002**, *146*, 20–23. [[CrossRef](#)]
45. Mantel, N.; Haenszel, W. Statistical Aspects of the Analysis of Data From Retrospective Studies of Disease. *J. Natl. Cancer Inst.* **1959**, *22*, 719–748.
46. Rozenberg, J.; Rishi, V.; Orosz, A.; Moitra, J.; Glick, A.; Vinson, C. Inhibition of CREB function in mouse epidermis reduces papilloma formation. *Mol. Cancer Res.* **2009**, *7*, 654–664. [[CrossRef](#)]
47. Tongkao-On, W.; Yang, C.; McCarthy, B.Y.; De Silva, W.G.M.; Rybchyn, M.S.; Gordon-Thomson, C.; Dixon, K.M.; Halliday, G.M.; Reeve, V.E.; Mason, R.S. Sex Differences in Photoprotective Responses to 1,25-Dihydroxyvitamin D<sub>3</sub> in Mice Are Modulated by the Estrogen Receptor-beta. *Int. J. Mol. Sci.* **2021**, *22*, 1962. [[CrossRef](#)]
48. Cooperstone, J.L.; Tober, K.L.; Riedl, K.M.; Teegarden, M.D.; Cichon, M.J.; Francis, D.M.; Schwartz, S.J.; Oberyszyn, T.M. Tomatoes protect against development of UV-induced keratinocyte carcinoma via metabolomic alterations. *Sci. Rep.* **2017**, *7*, 5106. [[CrossRef](#)]
49. Kripke, M.L.; Cox, P.A.; Alas, L.G.; Yarosh, D.B. Pyrimidine dimers in DNA initiate systemic immunosuppression in UV-irradiated mice. *Proc. Natl. Acad. Sci. USA* **1992**, *89*, 7516–7520. [[CrossRef](#)]
50. Damian, D.L.; Patterson, C.R.; Stapelberg, M.; Park, J.; Barnetson, R.S.; Halliday, G.M. UV radiation-induced immunosuppression is greater in men and prevented by topical nicotinamide. *J. Investig. Dermatol.* **2008**, *128*, 447–454. [[CrossRef](#)] [[PubMed](#)]
51. Reeve, V.E.; Allanson, M.; Domanski, D.; Painter, N. Gender differences in UV-induced inflammation and immunosuppression in mice reveal male unresponsiveness to UVA radiation. *Photochem. Photobiol. Sci.* **2012**, *11*, 173–179. [[CrossRef](#)] [[PubMed](#)]
52. Thomas-Ahner, J.M.; Wulff, B.C.; Tober, K.L.; Kusewitt, D.F.; Riggensbach, J.A.; Oberyszyn, T.M. Gender differences in UVB-induced skin carcinogenesis, inflammation, and DNA damage. *Cancer Res.* **2007**, *67*, 3468–3474. [[CrossRef](#)]

53. Foote, J.A.; Harris, R.B.; Giuliano, A.R.; Roe, D.J.; Moon, T.E.; Cartmel, B.; Alberts, D.S. Predictors for cutaneous basal- and squamous-cell carcinoma among actinically damaged adults. *Int. J. Cancer* **2001**, *95*, 7–11. [[CrossRef](#)] [[PubMed](#)]
54. Rees, J.R.; Zens, M.S.; Celaya, M.O.; Riddle, B.L.; Karagas, M.R.; Peacock, J.L. Survival after squamous cell and basal cell carcinoma of the skin: A retrospective cohort analysis. *Int. J. Cancer* **2015**, *137*, 878–884. [[CrossRef](#)] [[PubMed](#)]
55. Theil, J.H.; Ahloy-Dallaire, J.; Weber, E.M.; Gaskill, B.N.; Pritchett-Corning, K.R.; Felt, S.A.; Garner, J.P. The epidemiology of fighting in group-housed laboratory mice. *Sci. Rep.* **2020**, *10*, 16649. [[CrossRef](#)] [[PubMed](#)]
56. Deliconstantinos, G.; Villiotou, V.; Stavrides, J.C. Increase of particulate nitric oxide synthase activity and peroxy-nitrite synthesis in UVB-irradiated keratinocyte membranes. *Biochem. J.* **1996**, *320 Pt 3*, 997–1003. [[CrossRef](#)] [[PubMed](#)]
57. Villiotou, V.; Deliconstantinos, G. Nitric oxide, peroxy-nitrite and nitroso-compounds formation by ultraviolet A (UVA) irradiated human squamous cell carcinoma: Potential role of nitric oxide in cancer prognosis. *Anticancer. Res.* **1995**, *15*, 931–942.
58. Deliconstantinos, G.; Villiotou, V.; Stavrides, J.C. Release by ultraviolet B (u.v.B) radiation of nitric oxide (NO) from human keratinocytes: A potential role for nitric oxide in erythema production. *Br. J. Pharmacol.* **1995**, *114*, 1257–1265. [[CrossRef](#)]
59. Mowbray, M.; McLintock, S.; Weerakoon, R.; Lomatschinsky, N.; Jones, S.; Rossi, A.G.; Weller, R.B. Enzyme-Independent NO Stores in Human Skin: Quantification and Influence of UV Radiation. *J. Investig. Dermatol.* **2009**, *129*, 834–842. [[CrossRef](#)]
60. Urbanski, A.; Schwarz, T.; Neuner, P.; Krutmann, J.; Kirnbauer, R.; Kock, A.; Luger, T.A. Ultraviolet light induces increased circulating interleukin-6 in humans. *J. Investig. Dermatol.* **1990**, *94*, 808–811. [[CrossRef](#)]
61. Rossol, M.; Pierer, M.; Raulien, N.; Quandt, D.; Meusch, U.; Rothe, K.; Schubert, K.; Schoneberg, T.; Schaefer, M.; Krugel, U.; et al. Extracellular Ca<sup>2+</sup> is a danger signal activating the NLRP3 inflammasome through G protein-coupled calcium sensing receptors. *Nat. Commun.* **2012**, *3*, 1329. [[CrossRef](#)]
62. Gutierrez-Lopez, T.Y.; Orduna-Castillo, L.B.; Hernandez-Vasquez, M.N.; Vazquez-Prado, J.; Reyes-Cruz, G. Calcium sensing receptor activates the NLRP3 inflammasome via a chaperone-assisted degradative pathway involving Hsp70 and LC3-II. *Biochem. Biophys. Res. Commun.* **2018**, *505*, 1121–1127. [[CrossRef](#)]
63. Lee, G.S.; Subramanian, N.; Kim, A.I.; Aksentijevich, I.; Goldbach-Mansky, R.; Sacks, D.B.; Germain, R.N.; Kastner, D.L.; Chae, J.J. The calcium-sensing receptor regulates the NLRP3 inflammasome through Ca<sup>2+</sup> and cAMP. *Nature* **2012**, *492*, 123–127. [[CrossRef](#)]
64. Chiarini, A.; Armato, U.; Liu, D.; Dal Prà, I. Calcium-Sensing Receptor Antagonist NPS 2143 Restores Amyloid Precursor Protein Physiological Non-Amyloidogenic Processing in Aβ-Exposed Adult Human Astrocytes. *Sci. Rep.* **2017**, *7*, 1277. [[CrossRef](#)]
65. Armato, U.; Chiarini, A.; Chakravarthy, B.; Chioffi, F.; Pacchiana, R.; Colarusso, E.; Whitfield, J.F.; Dal Prà, I. Calcium-sensing receptor antagonist (calcilytic) NPS 2143 specifically blocks the increased secretion of endogenous Aβ<sub>42</sub> prompted by exogenous fibrillary or soluble Aβ<sub>25–35</sub> in human cortical astrocytes and neurons—Therapeutic relevance to Alzheimer’s disease. *Biochim. Biophys. Acta (BBA)-Mol. Basis Dis.* **2013**, *1832*, 1634–1652.
66. Zhai, T.Y.; Cui, B.H.; Zou, L.; Zeng, J.Y.; Gao, S.; Zhao, Q.; Wang, Y.; Xie, W.L.; Sun, Y.H. Expression and Role of the Calcium-Sensing Receptor in Rat Peripheral Blood Polymorphonuclear Neutrophils. *Oxid. Med. Cell. Longev.* **2017**, *2017*, 3869561. [[CrossRef](#)]
67. Li, T.T.; Sun, M.R.; Yin, X.; Wu, C.L.; Wu, Q.Y.; Feng, S.L.; Li, H.; Luan, Y.; Wen, J.; Yan, L.X.; et al. Expression of the calcium sensing receptor in human peripheral blood T lymphocyte and its contribution to cytokine secretion through MAPKs or NF-kappa B pathways (vol 53, pg 414, 2013). *Mol. Immunol.* **2013**, *55*, 429. [[CrossRef](#)]
68. Wu, C.-L.; Wu, Q.-Y.; Du, J.-J.; Zeng, J.-Y.; Li, T.-T.; Xu, C.-Q.; Sun, Y.-H. Calcium-sensing receptor in the T lymphocyte enhanced the apoptosis and cytokine secretion in sepsis. *Mol. Immunol.* **2015**, *63*, 337–342. [[CrossRef](#)] [[PubMed](#)]
69. Hu, B.; Tong, F.; Xu, L.; Shen, Z.; Yan, L.; Xu, G.; Shen, R. Role of Calcium Sensing Receptor in Streptozotocin-Induced Diabetic Rats Exposed to Renal Ischemia Reperfusion Injury. *Kidney Blood Press. Res.* **2018**, *43*, 276–286. [[CrossRef](#)]
70. Nishimura, N.; Tohyama, C.; Satoh, M.; Nishimura, H.; Reeve, V.E. Defective immune response and severe skin damage following UVB irradiation in interleukin-6-deficient mice. *Immunology* **1999**, *97*, 77–83. [[CrossRef](#)] [[PubMed](#)]
71. Murphy, G.M.; Norris, P.G.; Young, A.R.; Corbett, M.F.; Hawk, J.L.M. Low-dose ultraviolet-B irradiation depletes human epidermal Langerhans cells. *Br. J. Dermatol.* **1993**, *129*, 674–677. [[CrossRef](#)] [[PubMed](#)]
72. Aberer, W.; Schuler, G.; Stingl, G.; Honigsmann, H.; Wolff, K. Ultraviolet light depletes surface markers of Langerhans cells. *J. Investig. Dermatol.* **1981**, *76*, 202–210. [[CrossRef](#)] [[PubMed](#)]
73. Shreedhar, V.; Giese, T.; Sung, V.W.; Ullrich, S.E. A cytokine cascade including prostaglandin E<sub>2</sub>, IL-4, and IL-10 is responsible for UV-induced systemic immune suppression. *J. Immunol.* **1998**, *160*, 3783–3789. [[CrossRef](#)] [[PubMed](#)]
74. de Vries, J.E. Immunosuppressive and anti-inflammatory properties of interleukin 10. *Ann. Med.* **1995**, *27*, 537–541. [[CrossRef](#)]
75. Matsumura, Y.; Ananthaswamy, H.N. Toxic effects of ultraviolet radiation on the skin. *Toxicol. Appl. Pharmacol.* **2004**, *195*, 298–308. [[CrossRef](#)] [[PubMed](#)]
76. Rivas, J.M.; Ullrich, S.E. Systemic suppression of delayed-type hypersensitivity by supernatants from UV-irradiated keratinocytes. An essential role for keratinocyte-derived IL-10. *J. Immunol.* **1992**, *149*, 3865–3871. [[CrossRef](#)] [[PubMed](#)]
77. Yagi, H.; Tokura, Y.; Wakita, H.; Furukawa, F.; Takigawa, M. TCRV beta 7+ Th2 cells mediate UVB-induced suppression of murine contact photosensitivity by releasing IL-10. *J. Immunol.* **1996**, *156*, 1824–1831. [[CrossRef](#)]
78. Wolf, P.; Maier, H.; Mullegger, R.R.; Chadwick, C.A.; Hofmann-Wellenhof, R.; Soyer, H.P.; Hofer, A.; Smolle, J.; Horn, M.; Cerroni, L.; et al. Topical treatment with liposomes containing T4 endonuclease V protects human skin in vivo from ultraviolet-induced upregulation of interleukin-10 and tumor necrosis factor-alpha. *J. Investig. Dermatol.* **2000**, *114*, 149–156. [[CrossRef](#)]

79. Loser, K.; Apelt, J.; Voskort, M.; Mohaupt, M.; Balkow, S.; Schwarz, T.; Grabbe, S.; Beissert, S. IL-10 controls ultraviolet-induced carcinogenesis in mice. *J. Immunol.* **2007**, *179*, 365–371. [[CrossRef](#)] [[PubMed](#)]
80. You, Y.H.; Lee, D.H.; Yoon, J.H.; Nakajima, S.; Yasui, A.; Pfeifer, G.P. Cyclobutane pyrimidine dimers are responsible for the vast majority of mutations induced by UVB irradiation in mammalian cells. *J. Biol. Chem.* **2001**, *276*, 44688–44694. [[CrossRef](#)] [[PubMed](#)]
81. Yarosh, D.; Alas, L.G.; Yee, V.; Oberyszyn, A.; Kibitel, J.T.; Mitchell, D.; Rosenstein, R.; Spinowitz, A.; Citron, M. Pyrimidine Dimer Removal Enhanced by DNA Repair Liposomes Reduces the Incidence of UV Skin Cancer in Mice. *Cancer Res.* **1992**, *52*, 4227–4231. [[PubMed](#)]
82. Yarosh, D.; Klein, J.; O'Connor, A.; Hawk, J.; Rafal, E.; Wolf, P. Effect of topically applied T4 endonuclease V in liposomes on skin cancer in xeroderma pigmentosum: A randomised study. Xeroderma Pigmentosum Study Group. *Lancet* **2001**, *357*, 926–929. [[CrossRef](#)]
83. Gonzalez, G.A.; Montminy, M.R. Cyclic AMP stimulates somatostatin gene transcription by phosphorylation of CREB at serine 133. *Cell* **1989**, *59*, 675–680. [[CrossRef](#)]
84. Mayr, B.; Montminy, M. Transcriptional regulation by the phosphorylation-dependent factor CREB. *Nat. Rev. Mol. Cell Biol.* **2001**, *2*, 599–609. [[CrossRef](#)] [[PubMed](#)]
85. Conkright, M.D.; Montminy, M. CREB: The undicted cancer co-conspirator. *Trends Cell Biol.* **2005**, *15*, 457–459. [[CrossRef](#)] [[PubMed](#)]
86. Abramovitch, R.; Tavor, E.; Jacob-Hirsch, J.; Zeira, E.; Amariglio, N.; Pappo, O.; Rechavi, G.; Galun, E.; Honigman, A. A pivotal role of cyclic AMP-responsive element binding protein in tumor progression. *Cancer Res.* **2004**, *64*, 1338–1346. [[CrossRef](#)] [[PubMed](#)]
87. Melnikova, V.O.; Dobroff, A.S.; Zigler, M.; Villares, G.J.; Braeuer, R.R.; Wang, H.; Huang, L.; Bar-Eli, M. CREB Inhibits AP-2 alpha Expression to Regulate the Malignant Phenotype of Melanoma. *PLoS ONE* **2010**, *5*, e12452. [[CrossRef](#)]
88. Kim, S.Y.; Lee, J.H.; Sohn, K.C.; Im, M.; Lee, Y.; Seo, Y.J.; Lee, J.H.; Kim, C.D. beta-Catenin Regulates the Expression of cAMP Response Element-Binding Protein 1 in Squamous Cell Carcinoma Cells. *Ann. Dermatol.* **2018**, *30*, 119–122. [[CrossRef](#)]
89. Chhabra, A.; Fernando, H.; Watkins, G.; Mansel, R.E.; Jiang, W.G. Expression of transcription factor CREB1 in human breast cancer and its correlation with prognosis. *Oncol. Rep.* **2007**, *18*, 953–958. [[CrossRef](#)]
90. Jean, D.; Bar-Eli, M. Regulation of tumor growth and metastasis of human melanoma by the CREB transcription factor family. *Mol. Cell. Biochem.* **2000**, *212*, 19–28. [[CrossRef](#)]
91. Best, S.A.; Nwaobasi, A.N.; Schmults, C.D.; Ramsey, M.R. CCAR2 Is Required for Proliferation and Tumor Maintenance in Human Squamous Cell Carcinoma. *J. Invest. Dermatol.* **2017**, *137*, 506–512. [[CrossRef](#)]
92. Einspahr, J.G.; Curiel-Lewandrowski, C.; Calvert, V.S.; Stratton, S.P.; Alberts, D.S.; Warneke, J.; Hu, C.; Saboda, K.; Wagener, E.L.; Dickinson, S.; et al. Protein activation mapping of human sun-protected epidermis after an acute dose of erythemic solar simulated light. *NPJ Precis. Oncol.* **2017**, *1*, 34. [[CrossRef](#)]
93. Oh, W.J.; Rishi, V.; Orosz, A.; Gerdes, M.J.; Vinson, C. Inhibition of CCAAT/enhancer binding protein family DNA binding in mouse epidermis prevents and regresses papillomas. *Cancer Res.* **2007**, *67*, 1867–1876. [[CrossRef](#)]
94. Zhu, S.; Yoon, K.; Sterneck, E.; Johnson, P.F.; Smart, R.C. CCAAT/enhancer binding protein-beta is a mediator of keratinocyte survival and skin tumorigenesis involving oncogenic Ras signaling. *Proc. Natl. Acad. Sci. USA* **2002**, *99*, 207–212. [[CrossRef](#)]
95. Gerdes, M.J.; Myakishev, M.; Frost, N.A.; Rishi, V.; Moitra, J.; Acharya, A.; Levy, M.R.; Park, S.W.; Glick, A.; Yuspa, S.H.; et al. Activator protein-1 activity regulates epithelial tumor cell identity. *Cancer Res.* **2006**, *66*, 7578–7588. [[CrossRef](#)] [[PubMed](#)]
96. Young, M.R.; Li, J.J.; Rincon, M.; Flavell, R.A.; Sathyanarayana, B.K.; Hunziker, R.; Colburn, N. Transgenic mice demonstrate AP-1 (activator protein-1) transactivation is required for tumor promotion. *Proc. Natl. Acad. Sci. USA* **1999**, *96*, 9827–9832. [[CrossRef](#)] [[PubMed](#)]
97. Thompson, E.J.; MacGowan, J.; Young, M.R.; Colburn, N.; Bowden, G.T. A dominant negative c-jun specifically blocks okadaic acid-induced skin tumor promotion. *Cancer Res.* **2002**, *62*, 3044–3047. [[PubMed](#)]
98. Bikle, D.D.; Oda, Y.; Tu, C.L.; Jiang, Y. Novel mechanisms for the vitamin D receptor (VDR) in the skin and in skin cancer. *J. Steroid Biochem.* **2015**, *148*, 47–51. [[CrossRef](#)]
99. Bikle, D.D.; Jiang, Y.; Nguyen, T.; Oda, Y.; Tu, C.L. Disruption of Vitamin D and Calcium Signaling in Keratinocytes Predisposes to Skin Cancer. *Front. Physiol.* **2016**, *7*, 296. [[CrossRef](#)]
100. Panich, U.; Sittithumcharee, G.; Rathviboon, N.; Jirawatnotai, S. Ultraviolet Radiation-Induced Skin Aging: The Role of DNA Damage and Oxidative Stress in Epidermal Stem Cell Damage Mediated Skin Aging. *Stem Cells Int.* **2016**, *2016*, 7370642. [[CrossRef](#)]
101. Reeve, V.E.; Domanski, D.; Slater, M. Radiation sources providing increased UVA/UVB ratios induce photoprotection dependent on the UVA dose in hairless mice. *Photochem. Photobiol.* **2006**, *82*, 406–411. [[CrossRef](#)]
102. Rybchyn, M.S.; Slater, M.; Conigrave, A.D.; Mason, R.S. An Akt-dependent increase in canonical Wnt signaling and a decrease in sclerostin protein levels are involved in strontium ranelate-induced osteogenic effects in human osteoblasts. *J. Biol. Chem.* **2011**, *286*, 23771–23779. [[CrossRef](#)] [[PubMed](#)]
103. De Silva, W.G.M.; Han, J.Z.R.; Yang, C.; Tongkao-On, W.; McCarthy, B.Y.; Ince, F.A.; Holland, A.J.A.; Tuckey, R.C.; Slominski, A.T.; Abboud, M.; et al. Evidence for Involvement of Nonclassical Pathways in the Protection From UV-Induced DNA Damage by Vitamin D-Related Compounds. *JBMIR Plus* **2021**, *5*, e10555. [[CrossRef](#)]

104. Dell, R.B.; Holleran, S.; Ramakrishnan, R. Sample size determination. *ILAR J.* **2002**, *43*, 207–213. [[CrossRef](#)] [[PubMed](#)]
105. Schmidt, S.A.J.; Lo, S.; Hollestein, L.M. Research Techniques Made Simple: Sample Size Estimation and Power Calculation. *J. Investig. Dermatol.* **2018**, *138*, 1678–1682. [[CrossRef](#)] [[PubMed](#)]

**Disclaimer/Publisher's Note:** The statements, opinions and data contained in all publications are solely those of the individual author(s) and contributor(s) and not of MDPI and/or the editor(s). MDPI and/or the editor(s) disclaim responsibility for any injury to people or property resulting from any ideas, methods, instructions or products referred to in the content.